

Exploiting Non-uniform Quantization for Enhanced ILC in Wideband Digital Pre-distortion

Jinfei Wang¹, Yi Ma^{1†}, Fei Tong², and Ziming He²

¹5GIC and 6GIC, Institute for Communication Systems, University of Surrey, Guildford, UK, GU2 7XH

[†]Emails: (jinfei.wang, y.ma, r.tafazolli@surrey.ac.uk)

²Samsung Cambridge Solution Centre, Cambridge, UK, CB4 0AE

²Emails: (f.tong, ziming.he@samsung.com)

Abstract—In this paper, it is identified that lowering the reference level at the vector signal analyzer can significantly improve the performance of iterative learning control (ILC). We present a mathematical explanation for this phenomenon, where the signals experience logarithmic transform prior to analogue-to-digital conversion, resulting in non-uniform quantization. This process reduces the quantization noise of low-amplitude signals that constitute a substantial portion of orthogonal frequency division multiplexing (OFDM) signals, thereby improving ILC performance. Measurement results show that compared to setting the reference level to the peak amplitude, lowering the reference level achieves 3 dB improvement on error vector magnitude (EVM) and 15 dB improvement on normalized mean square error (NMSE) for 320 MHz WiFi OFDM signals.

Index Terms—Digital pre-distortion (DPD), iterative learning control (ILC), wideband, reference level.

I. INTRODUCTION

Iterative learning control (ILC) has gained significant attention in digital pre-distortion (DPD) for identifying optimal input signals to the power amplifier (PA) for its excellent robustness to the memory effects and non-linearity of PAs [1]–[5]. However, the performance of ILC is highly dependent on the signal-to-noise ratio (SNR) of the captured PA output signals [6]. This challenge is particularly critical for wideband signals with pronounced memory effects.

In this paper, it is identified that lowering the reference level of the vector signal analyzer (VSA) can significantly improve ILC performance. We present a mathematical explanation for this phenomenon. When the reference level is lower than the peak signal amplitude, the signals experience logarithmic transform before passing the analogue-to-digital converter (ADC), resulting in non-uniform quantization. This reduces the quantization step size for low-amplitude signals while relaxing it for high-amplitude signals, thereby reducing the quantization noise for low-amplitude components. This property is particularly beneficial for orthogonal frequency-division multiplexing (OFDM) signals, as small-amplitude components constitute a substantial portion of OFDM signals.

Measurement results show that lowering the reference level by more than 17 dB compared to the peak amplitude yields a 3 dB improvement on error vector magnitude (EVM) and a 15 dB improvement on normalized mean square error (NMSE) for WiFi OFDM signals with bandwidths of 160 MHz and

320 MHz. Specifically, the ILC achieves $-49 \sim -46$ dB EVM and up to -54 dB NMSE, demonstrating competitive performance compared to the literature (e.g., [1]–[5]). Moreover, employing generalized memory polynomial (GMP) models to fit the ILC results achieves comparable EVM performance to the ILC and $-46 \sim -43$ dB NMSE. These findings confirm that lowering the VSA reference level is a simple yet effective approach to enhancing ILC performance, particularly for wideband OFDM signals.

II. PRINCIPLE OF ILC

Consider an OFDM signal $\mathbf{s} \in \mathbb{C}^{N \times 1}$. Ideally, we hope the output of the PA output $\mathbf{y} \in \mathbb{C}^{N \times 1}$ is a linearly amplified version of \mathbf{s} . However, due to the inherent non-linearity and memory effects of the PA, this ideal behavior is not easily achieved in practice. The aim of DPD design is to mitigate these imperfections. Denote the PA function by $f(\cdot)$ and the DPD function by $g(\cdot)$. Then, the target of DPD is to find $g(\cdot)$ such that

$$\mathbf{y} = f(g(\mathbf{s})) = G\mathbf{s}, \quad (1)$$

where $G > 1$ stands for the PA gain.

Since the PA function $f(\cdot)$ is generally unknown, it is challenging to directly determine $g(\cdot)$. Various methods have been proposed to handle this issue, e.g., [7]–[9]. Among these, ILC has emerged as a promising approach, achieving impressive performance without requiring explicit modeling of $f(\cdot)$ or $g(\cdot)$ [10]. The idea of ILC is to directly acquire PA input signal \mathbf{x} through iterative feedback such that

$$f(\mathbf{x}) = G\mathbf{s}. \quad (2)$$

To facilitate the discussion in the subsequent section, the principle of ILC with linear update is elaborated as follows. Note that the discussion in the next section is also applicable to the gain-inverse update. Denote the PA input and output of the i -th ILC iteration by \mathbf{x}_i and \mathbf{y}_i ($i = 0, 1, \dots$), respectively. The process begins with the initial PA input:

$$\mathbf{x}_0 = \mathbf{s}. \quad (3)$$

In each iteration, the ILC signal is updated as

$$\mathbf{x}_{i+1} = \mathbf{x}_i + \mathbf{e}_i, \quad (4)$$

where the update error \mathbf{e}_i is defined as

$$\mathbf{e}_i \triangleq \mathbf{y}_i - \mathbf{s}. \quad (5)$$

According to [10], we will have the following equation after enough iterations:

$$\lim_{n \rightarrow \infty} f(\mathbf{x}_i) = G\mathbf{s}. \quad (6)$$

In practice, \mathbf{y}_i usually converge close to $G\mathbf{s}$ within 10 iterations [5], [6].

III. NON-UNIFORM QUANTIZATION FOR ILC FEEDBACK

The convergence analysis of ILC in [10] was based on the assumption that \mathbf{y}_i is exactly the PA output. In practice, \mathbf{y}_i is captured by the VSA before the update (5) happens. This process involves multiple parameters, such as ADC quantization, ADC sampling rate, fractional delay compensation and thermal noise. In this paper, we focus on the mathematical explanation using the ADC quantization for the ILC performance with respect to the reference level.

Our testbed measurements in Section V reveal that setting the reference level below the peak signal amplitude can significantly improve ILC performance, even though it is commonly recommended to set the reference level above the peak signal amplitude. It is likely that the signals undergoes a logarithmic transform prior to uniform quantization [11]. Motivated by these observations, we aim to provide a mathematical explanation for the measurement results.

Assume that the quantization process for the in-phase and quadrature part of \mathbf{y}_i is performed independently, and the quantization of positive and negative values is symmetric [11]. Hence, we are interested in the quantization of $|\Re(\mathbf{y}_i)|$, where $\Re(\cdot)$ stands for the real part of a scalar/vector, $|\cdot|$ for the absolute value of a scalar/vector. This quantization problem can be linearly scaled to the quantization of \mathbf{z}_i :

$$z_i(n) = |\Re(y_i(n))|/y_{i,\max}, \quad (7)$$

where

$$y_{i,\max} = \max_n |\Re(y_i(n))|. \quad (8)$$

It is trivial that $z_i(n) \in [0, 1]$. Consider this interval to be divided into $(Q + 1)$ intervals ($Q \in \mathbb{N}^+$). Denote the q -th quantization thresholds by d_q ($q = 1, \dots, Q$). The quantization step, denoted by δ_q , is defined as

$$\delta_q \triangleq d_{q+1} - d_q, \quad q = 1, 2, \dots, Q - 1. \quad (9)$$

In the case of uniform quantization, we have

$$d_q = q/(Q + 1), \quad \delta_q = 1/(Q + 1). \quad (10)$$

Mathematically, we are looking for a logarithmic transform function $h(z_i(n))$, where uniform quantization is applied to $h(z_i(n))$. To facilitate our analysis, denote the ratio of $y_{i,\max}$ over current reference level by ρ ($\rho > 1$). $h(z_i(n))$ should satisfy the following two conditions: 1) $\delta_q < \delta_{q+1}$; 2) δ_q decreases with the increase of ρ for low-amplitude signals. This leads to the following theoretical result.

TABLE I
TESTBED PARAMETERS

Parameter	Value
DAC rate	960 MHz
ADC rate	640 MHz
DAC resolution	12-bit
ADC resolution	12-bit
Carrier Frequency	5.32 GHz
OFDM Signal Bandwidth	160 & 320 MHz

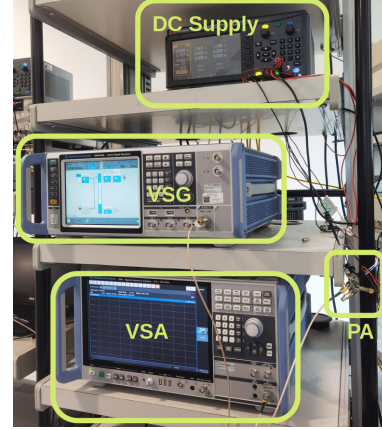


Fig. 1. Testbed setup.

Theorem 1: A logarithmic transform that satisfy the aforementioned two conditions is

$$h(z_i(n)) \triangleq \log_\rho((\rho - 1)z_i(n) + 1). \quad (11)$$

Proof: $h(z_i(n))$ in (11) is monotonically increasing with $z_i(n)$. Since $z_i(n) \in [0, 1]$, it follows that $h(z_i(n))$ falls in $[0, 1]$ as well. Then, when uniform quantization is applied to $h(z_i(n))$, the quantization thresholds are already given by (10).

To know the equivalent quantization threshold d_q for $z_i(n)$, we have the following equation:

$$q/(Q + 1) = \log_\rho((\rho - 1)d_q + 1). \quad (12)$$

Solving (12) yields

$$d_q = (\rho^{q/(Q+1)} - 1)/(\rho - 1). \quad (13)$$

Hence, we have

$$\delta_q = \frac{\rho^{q/(Q+1)}(\rho^{1/(Q+1)} - 1)}{\rho - 1} \quad (14)$$

$$= \frac{\rho^{q/(Q+1)}}{\sum_{k=1}^{k=Q} \rho^{k/(Q+1)}}. \quad (15)$$

Since the numerator in (15) increases with the increase of q , we have $\delta_q < \delta_{q+1}$. Moreover, as ρ increases, $\rho^{k/(Q+1)}$ is increasing faster with the increase of k . Therefore, δ_q decreases with the increase of ρ when q is small, i.e., for low amplitude signals. *Theorem 1* is proved. ■

Theorem 1 provides a theoretical explanation for phenomenon to be demonstrated later in Section V. By introducing smaller quantization step sizes for low-amplitude signals, the associated quantization noise is reduced [12]. This results

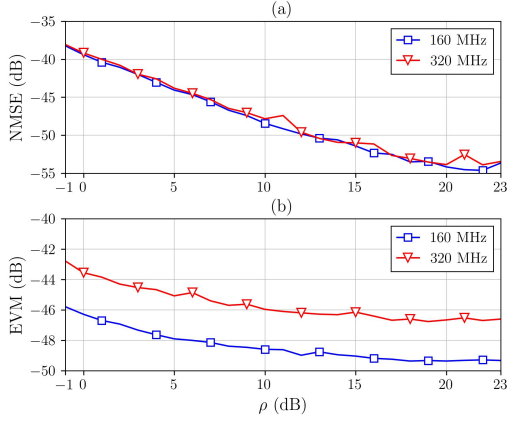


Fig. 2. NMSE and EVM of ILC with respect to the ratio of signal peak amplitude over reference level (i.e., ρ).

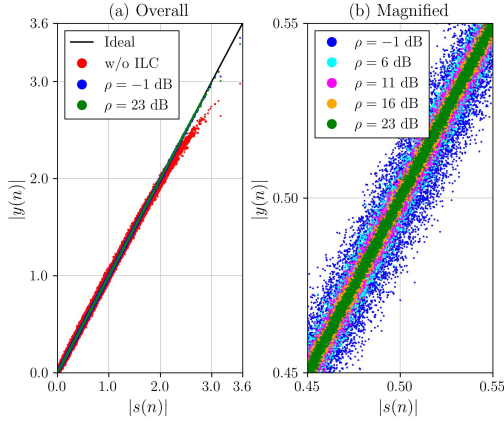


Fig. 3. Overall and magnified AM-AM behavior of ILC with respect to the change of ρ for 320 MHz WiFi OFDM signals.

in an improved SNR for the ILC feedback of OFDM signals, thereby enhancing ILC performance.

Although *Theorem 1* could not be explicitly verified in the VSA, it also provides theoretical insight for the design of VSA to improve the ILC performance, and consequently improves DPD performance.

IV. MEASUREMENT RESULTS AND DISCUSSION

In this section, we present the testbed setup and the results of our experiments. The testbed consists of a Rhode & Schwarz SMM100A vector signal generator (VSG), a Rhode & Schwarz FSW VSA, and a Qorvo QM45500 PA in low-power mode, as shown in Fig.1. Detailed testbed parameters are provided in Table I. The WiFi OFDM signals used in the experiments have a peak-to-average power ratio (PAPR) of 11 dB.

Experiment 1: The aim of this experiment is to demonstrate the change of ILC performance with respect to the VSA reference level, as shown in Fig. 2~Fig. 4.

Fig. 2 demonstrates the NMSE and EVM of ILC as the ratio of peak signal amplitude over the reference level ρ increases from -1 dB to 23 dB. We start the test from $\rho = -1$ dB as this is the commonly suggested setup: the reference level is

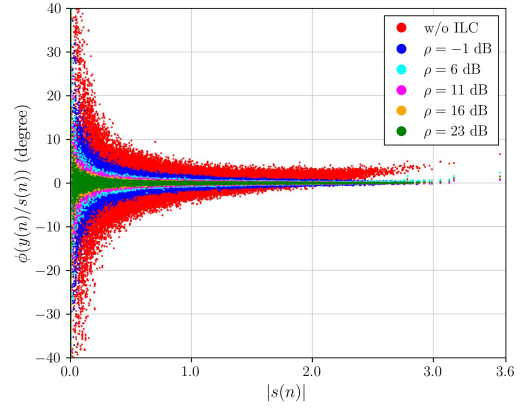


Fig. 4. AM-PM behavior of ILC with respect to the change of ρ for 320 MHz WiFi OFDM signals.

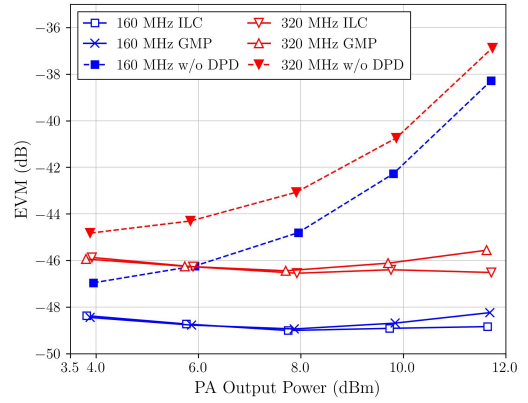


Fig. 5. EVM of ILC and GMP with the increase of PA output power for 160 MHz and 320 MHz WiFi OFDM signals.

slightly higher than the peak signal amplitude. Both the NMSE and EVM, increasing ρ significantly improves the NMSE for 15 dB and EVM for 3 dB as shown in Fig. 2(a) and Fig. 2(b), respectively.

The NMSE performance in Fig. 2(a) shows some swinging behavior. This is likely due to the resolution of fractional delay compensation is 32 in our experiment. This may not be fully sufficient for NMSE of -50 dB or less.

Fig. 3 shows the AM-AM behavior with respect to the change of ρ . Specifically, Fig. 3(a) shows the overall AM-AM behavior, where changing ρ does not seem to introduce significant difference. But when the AM-AM behavior is magnified, as in Fig. 3(b), it is observed that increasing ρ significantly reduces the memory effects for low-amplitude signals. Similar phenomenon is observed in the AM-PM behavior, as shown in Fig. 4.

It is also observed that when $\rho = 16$ dB, it already achieves close performance to the case when $\rho = 23$ dB in Fig. 2~Fig. 4. In *Experiment 2*, we will use the setting that $\rho = 16$ dB.

Experiment 2: The aim of this experiment is to demonstrate the DPD performance when using GMP (see [13]) to fit ILC results. To this end, the least-square fitting is adopted [13].

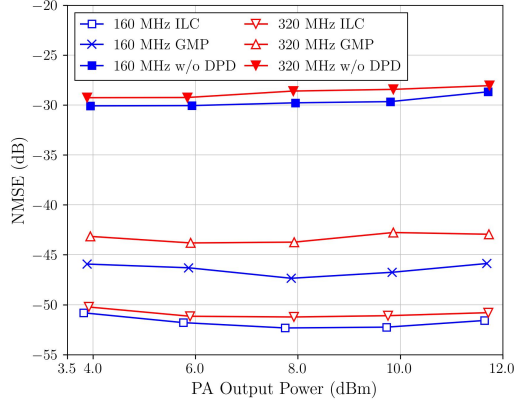


Fig. 6. NMSE of ILC and GMP with the increase of PA output power for 160 MHz and 320 MHz WiFi OFDM signals.

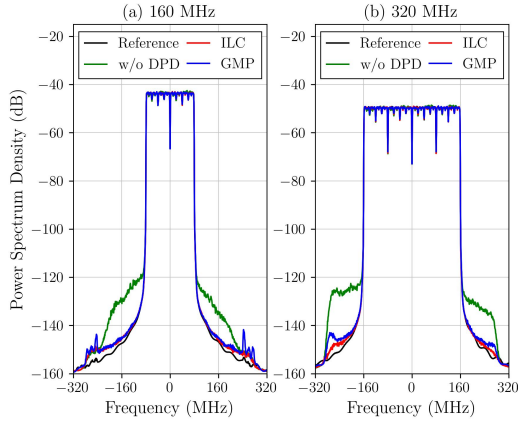


Fig. 7. PSD of ILC and GMP when the PA output power is 11.8 dBm for 160 MHz and 320 MHz WiFi OFDM signals.

The experiment is based on 100 waveforms in the training dataset as well as 100 waveforms in the test dataset.

For the GMP, the maximum memory depth is 20; the cross-memory depth is 1. The polynomial order gradually increases from 3 to 9 with the increase of PA output power.

Fig. 5 demonstrates the EVM as the PA output power increases. The GMP achieves almost identical EVM performance to the ILC (less than 1 dB performance degradation). For the NMSE, as shown in Fig. 6, there is around 5 dB degradation compared to the ILC. But the GMP still achieves -43 dB NMSE. This shows the performance improvement of ILC effectively transforms into the improvement on DPD performance. The average NMSE in Fig. 6 is worse than Fig. 2, this is due to the swinging phenomenon noted in Fig. 2, which may stem from insufficient fractional delay compensation.

Finally, Fig. 7 shows the power spectrum density (PSD) of ILC and GMP. Both the GMP and ILC are close to the reference signal, with limited out-of-band emissions. Notably, ILC still achieves good performance when the ADC rate is limited, as in Fig. 7(b). This is encouraging for the application of ILC in wideband DPD.

V. CONCLUSION

In this paper, it has been identified that lowering the reference level at the VSA significantly enhances ILC performance. A mathematical explanation has been provided for this phenomenon, where the signals undergo a logarithmic transformation prior to uniform quantization. This effectively reduces the quantization steps as well as quantization noise for low-amplitude signals. Measurement results have shown that lowering the reference level improves the NMSE by 15 dB and the EVM by 3 dB for 160 ~ 320 MHz WiFi OFDM signals, achieving up to -55 dB NMSE and -49 ~ -46 dB EVM. These improvements effectively transforms into DPD performance enhancement when employing the GMP fitting model.

ACKNOWLEDGEMENT

This work is funded by Samsung-Academy Global Collaborative Research Programme. Our sincere appreciation to Zern C. Tay and Jacob Sharpe for their outstanding support on testbed measurements.

REFERENCES

- [1] J. Peng, W. Shi, J. Pang, F. You, and S. He, "Iterative learning control for signal separation in dual-RF input Doherty transmitter," in *Proc. Eur. Microw. Conf. (EuMC)*, 2021, pp. 953–956.
- [2] X. Xia, Y. Liu, C. Li, W. Guo, C. Shi, S. Shao, L. Lei, and Y. Tang, "A high-accuracy digital predistorter constructed by reproducing iterations of ILC with cascade architecture," in *Proc. IEEE MTT-S Int. Microw. Symp. (IMS)*, 2021, pp. 446–449.
- [3] A. Fawzy, S. Sun, T. J. Lim, Y. X. Guo, and P. H. Tan, "Iterative learning control for pre-distortion design in wideband direct-conversion transmitters," in *Proc. IEEE Global Commun. Conf. (GLOBECOM)*, 2020, pp. 1–6.
- [4] S. Wang, W. Cao, and T. Eriksson, "Identification methods with different digital predistortion models for power amplifiers with strong nonlinearity and memory effects," in *Proc. IEEE MTT-S Int. Wireless Symp. (IWS)*, 2020, pp. 1–3.
- [5] A. Fawzy, S. Sun, T. J. Lim, Y. Yu, C. Yu, and Y. Guo, "Iterative learning control based digital pre-distortion for mitigating impairments in MIMO wireless transmitters," *IEEE Trans. Veh. Technol.*, vol. 72, no. 6, pp. 6933–6947, June 2023.
- [6] J. Chani-Cahuana, M. Özen, C. Fager, and T. Eriksson, "Digital pre-distortion parameter identification for RF power amplifiers using real-valued output data," *IEEE Trans. Circuits Syst. II: Exp. Briefs*, vol. 64, no. 10, pp. 1227–1231, Oct. 2017.
- [7] C. Eun and E. Powers, "A new Volterra predistorter based on the indirect learning architecture," *IEEE Trans. Signal Process.*, vol. 45, no. 1, pp. 223–227, Jan. 1997.
- [8] C. Liu, L. Luo, J. Wang, C. Zhang, and C. Pan, "A new digital predistortion based on B spline function with compressive sampling pruning," in *Proc. Int. Wireless Commun. Mobile Comput. (IWCMC)*, 2022, pp. 1200–1205.
- [9] Z. He and F. Tong, "Residual RNN models with pruning for digital predistortion of RF power amplifiers," *IEEE Trans. Veh. Technol.*, vol. 71, no. 9, pp. 9735–9750, Sept. 2022.
- [10] J. Chani-Cahuana, P. N. Landin, C. Fager, and T. Eriksson, "Iterative learning control for RF power amplifier linearization," *IEEE Trans. Microw. Theory Techn.*, vol. 64, no. 9, pp. 2778–2789, July 2016.
- [11] S. Pavan, R. Schreier, and G. Temes, *Understanding delta-sigma data converters*. Wiley & Sons, 2016.
- [12] L. Liu, Y. Ma, and N. Yi, "Hermite expansion model and LMMSE analysis for low-resolution quantized MIMO detection," *IEEE Trans. Signal Process.*, vol. 69, pp. 5313–5328, Sept. 2021.
- [13] D. Morgan, Z. Ma, J. Kim, M. Zierdt, and J. Pastalan, "A generalized memory polynomial model for digital predistortion of RF power amplifiers," *IEEE Trans. Signal Process.*, vol. 54, no. 10, pp. 3852–3860, Oct. 2006.